Journal of Magnetic Resonance **151,** 291–297 (2001)
doi:10.1006/jmre.2001.2384, available online at http://www.idealibrary.com on IDEAL®

NMR Relaxation and Diffusion Measurements on Iron(III)-Doped Kaolin Clay

R. M. E. Valckenborg, L. Pel, and K. Kopinga

Department of Applied Physics, Eindhoven University of Technology, P.O. Box 513, 5600 MB Eindhoven, The Netherlands

Received December 19, 2000; revised May 11, 2001; published online July 6, 2001

Kaolin clay samples were mixed with various amounts of Fe_2O_3 powder. The influence of this magnetic impurity on NMR relaxation and diffusion measurements on the water in this porous material was investigated. The NMR relaxation measurements showed a nearly mono-exponential decay, leading to the conclusion that the pore size distribution of the clay samples is either narrow and/or that the pores are interconnected very well. Both the longitudinal and the transverse relaxation rate depend linearly on the concentration of the Fe_2O_3 impurity. The NMR diffusion measurements revealed that the Fe_2O_3 causes internal magnetic field gradients that largely exceed the maximum external gradient that could be applied by our NMR apparatus (0.3 T/m). Additional SQUID measurements yielded the magnetization and magnetic susceptibility of the samples at the magnetic field strength used in the NMR measurements (0.8 T). A theoretical estimate of the internal magnetic field gradients leads to the conclusion that the water in the porous clay samples cannot be described by the commonly observed motional averaging regime. Probably an intermediate or a localization regime is induced by the large internal gradients, which are estimated to be on the order of 1 to 10 T/m in the pore volume and may exceed 1000 T/m at the pore surface.

Key Words: **NMR relaxometry; NMR diffusometry; Kaolin clay; magnetization; magnetic susceptibility; effective magnetic field gradients.**

1. INTRODUCTION

Nuclear Magnetic Resonance (NMR) on hydrogen (^{1}H) of water has become a general tool for determining pore size distributions of water saturated porous materials (*1*). Among the porous materials of interest are brick (*2*), mortar (*3*), silica-gels (*1*), and rock (*4*). The materials with the highest concentrations of magnetic impurities (about 10 wt%) are the most difficult to measure, because the magnetic field gradients resulting from these impurities dephase the NMR signal very rapidly. Our interest is directed to porous building materials, which do have these high concentrations of magnetic impurities. The objective of this research is to investigate quantitatively the effect of magnetic impurities on the NMR transverse (T_2) and longitudinal (T_1) relaxation times. Also their effect on the NMR diffusion measurements is investigated. To this end a series of Kaolin clay samples with different concentrations of magnetic impurities has been prepared. First, the sample preparation and characterization will be described, after which the NMR relaxation and diffusion measurements are presented.

2. MAGNETIC IMPURITIES

In order to study the effect of magnetic impurities on NMR relaxation and diffusion measurements, a series of specific samples has been chosen. We will first discuss the exact sample choice and preparation. Next, the field dependence of the magnetization of these samples will be presented.

2.1. Sample Preparation

In the present study, a mixture of dry Kaolin clay powder and Fe_2O_3 powder is used for the sample preparation. The clay powder and the Fe_2O_3 powder were thoroughly mixed. Next, water was added. The samples were not compacted, but defined as water saturated at the water concentration at which they just started to swell. The Kaolin clay powder consists of aluminum calcium silicates ($AlCaSiO_3$). The Fe_2O_3 concentration was varied between 0 and about 10 wt%. From a PIDS (particle size determination with light scattering) measurement the size of the clay powder particles and the particle size of the Fe_2O_3 were determined. It was found that the particle size of the clay is about 10 μm and that the mean particle size of the Fe_2O_3 is about 1 μm. We assume that the typical pore size is of the same order as the typical particle size. This gives an approximate pore size of 1 to 10 μm. Additional SEM images confirm this assumption, although also a few pores larger than 10 μm were observed.

2.2. Magnetization

The magnetization of the prepared clay samples has been measured with a SQUID-magnetometer. This very sensitive device measures the magnetization as a function of the applied magnetic field.

Figure 1 shows the result of a SQUID measurement on a clay sample with 4.3 wt% Fe_2O_3. The sample appears to have both a ferromagnetic and a paramagnetic magnetization. The paramagnetic contribution is characterized by a straight line with a positive slope, so the magnetization of the sample increases

1090-7807/01 $35.00

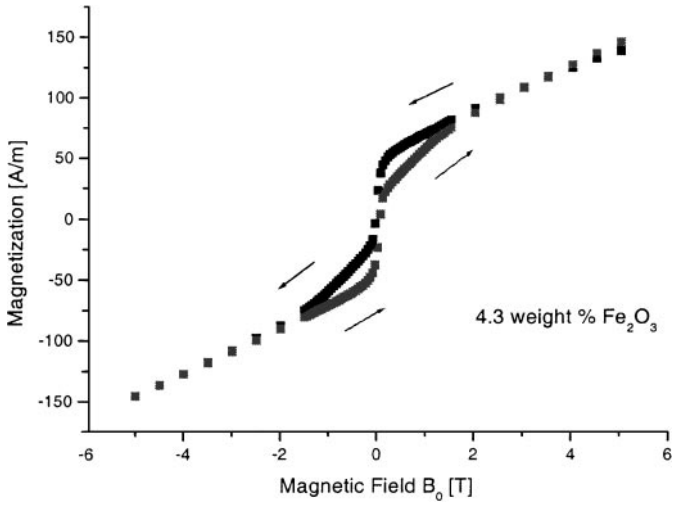

FIG. 1. Magnetization of impurity doped Kaolin clay as a function of the magnetic field. The arrows denote the direction of the magnetic field sweep.

at increasing magnetic fields. The ferromagnetic contribution is characterized by the hysteresis loop around zero magnetic field. The NMR-measurements were performed at $B_0 = 0.8$ T. At this magnetic field strength, the magnetization is obviously a combination of a ferromagnetic and a paramagnetic contribution.

SQUID measurements on all samples revealed that both the ferromagnetic magnetization (in Bohr-magnetons) and the paramagnetic magnetization depend linearly on the amount of Fe_2O_3 impurities. Only the pure Kaolin clay sample had no ferromagnetic magnetization. For the NMR experiments, the magnetization is the relevant property, since that is directly related to the internal magnetic field gradients in the sample. For paramagnetism, this magnetization is described adequately by a magnetic susceptibility χ, like is common in NMR literature. For ferromagnetism, however, the magnetic susceptibility is a function of magnetic field strength and not a logical parameter to describe the magnetic properties of the porous material. Therefore, in this paper the magnetization M of the porous material is used and not the magnetic susceptibility. Figure 2 shows the total magnetization of our samples at $B_0 = 0.8$ T as a function of the amount of Fe_2O_3.

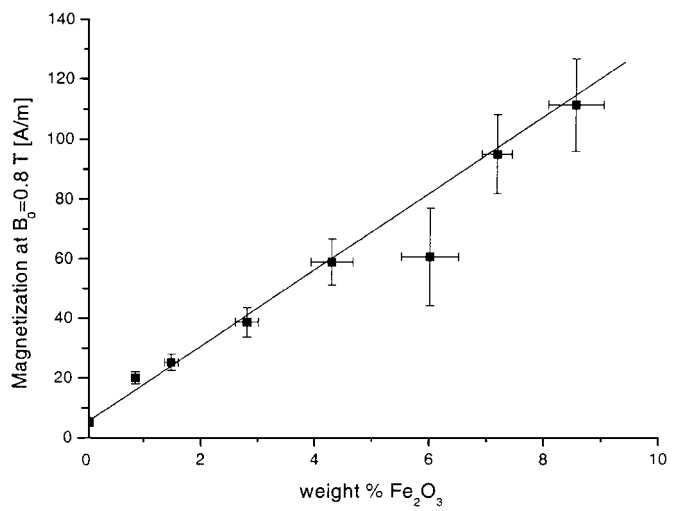

FIG. 2. Magnetization of impurity doped Kaolin clay at $B_0 = 0.8$ T. The line represents a linear fit through the data.

3. RELAXATION

The total transverse signal decay $\exp(-t/T_{2,tot})$ in a NMR spin echo experiment will be divided into two parts $T_{2,r}$ and $T_{2,d}$:

$$\frac{1}{T_{2,tot}} = \frac{1}{T_{2,r}} + \frac{1}{T_{2,d}}. \qquad [1]$$

In the term $T_{2,r}$ all relaxation mechanisms are included, i.e., both the bulk relaxation and the relaxation at the surface of the pore wall. The molecular self diffusion, the pore size, and the magnetic properties of the pore wall determine whether $T_{2,r}$ will be in the so-called slow or fast diffusion limit (*5*, *6*). The term $T_{2,d}$, on the other hand, reflects the dephasing due to random motion in the presence of a magnetic field gradient.

Because the longitudinal magnetization cannot dephase, it can be written as

$$\frac{1}{T_{1,tot}} = \frac{1}{T_{1,r}}. \qquad [2]$$

Within this formalism, the transverse magnetization $M(t)$ observed by a Hahn spinecho sequence can be described by

$$M(t) = M_0 \exp\left(-\frac{t}{T_{2,tot}}\right) = M_0 \exp\left(-\frac{t}{T_{2,r}}\right) \cdot E_d, \qquad [3]$$

where M_0 is the magnetization in equilibrium and E_d describes the signal decay due to dephasing effects. In a bulk fluid, the latter term is often referred to as the signal decay due to self-diffusion (*7*). One should note, however, that in a porous system this terminology may be somewhat confusing, since in that case the self-diffusion also has an effect on $T_{2,r}$.

The contribution of $T_{2,r}$ to the total transverse relaxation time $T_{2,tot}$ of the samples was measured with a CPMG pulse sequence (*8*). In order to minimize dephasing effects, the time between successive 180° pulses was taken as small as possible, which is 160 μs for our experimental setup. The assumption that dephasing effects do not affect the measurements with this pulse sequence was checked by doing also CPMG measurements with an interpulse time of 320, 640, 1280, and 2560 μs. Of course, the decay is largest for the measurement with the largest interpulse time. We observed that especially the decay curves of the samples with high impurity concentrations were not mono-exponential. The data for each individual sample were

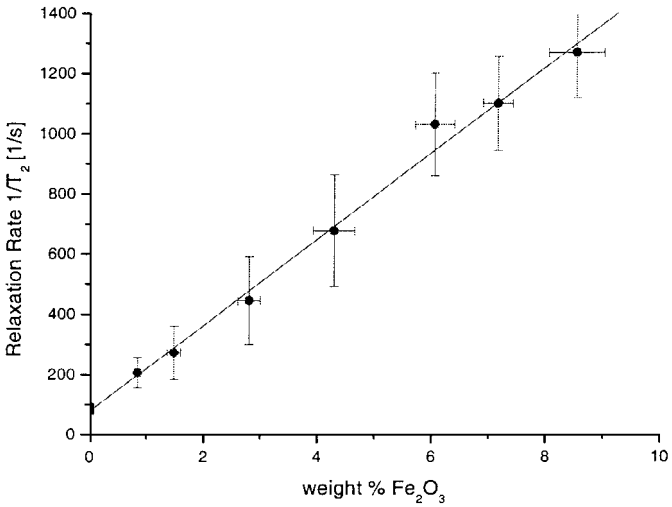

FIG. 3. Transverse relaxation rate as a function of the amount of magnetic impurities.

extrapolated to yield the limiting situation of a CPMG measurement with zero interpulse time. The resulting curves were found to match the results obtained with 160 μs interpulse time rather closely. It is also possible to fit the beginning of the decay curve with a mono-exponential function. The decay constant of this fit will be called $T_{2,CPMG}$. A plot of this "short-time CPMG behavior" decay constant as a function of interpulse time can be used to extrapolate the data to zero interpulse time. Various extrapolation schemes yield nearly the same decay constant as the 160 μs interpulse time experiment. Figure 3 shows the inverse of the relaxation time $T_{2,r}$ for an interpulse time of 160 μs as a function of the wt% Fe_2O_3.

The longitudinal relaxation time T_1 was measured with a saturation recovery measurement (*9*). The time between the 90° and 180° pulses was set at a constant value of 80 μs, effectively eliminating dephasing and transverse relaxation effects. The T_1 relaxation appeared to be perfectly mono-exponential, indicating that the pore fluid is in the so-called "fast diffusion limit"(*5*). If the pores in our clay material are not of exactly the same size, the behavior of T_1 suggests that they are interconnected so well that diffusion averages out all structure effects (*10*) which are smaller than the average pore size.

Figure 4 shows the inverse of the relaxation time T_1 as a function of the wt% Fe_2O_3. Inspection of Figs. 3 and 4 reveals that both the transverse and longitudinal relaxation rate increase linearly with the magnetic impurity content.

Because the typical pore size ($l_S \sim V/S$) is about the same for all samples and because the pores are in the fast diffusion limit, the relaxation rate can be translated to a surface relaxivity ρ using the relation (*1*)

$$\rho_i = \frac{1}{T_{i,r}} \cdot \frac{V}{S}. \qquad [4]$$

The subscript $i = 1, 2$ denotes either longitudinal or transverse relaxation. Given the results presented in Figs. 3 and 4, this implies that the surface relaxivity ρ varies linearly with the wt% Fe_2O_3. The relatively high longitudinal relaxation rate of the pure clay sample (at 0% Fe_2O_3 in Fig. 4) can be explained by the magnetism of natural Kaolin clay, which causes an enhanced surface relaxivity ρ_1. This effect is reported extensively by Bryar *et al.* (*11*).

Figure 4 shows that adding more magnetic impurities to the Kaolin clay does increase the surface relaxivity, but not by more than one order of magnitude. On the other hand, the transverse relaxation rate of the pure Kaolin clay increases dramatically when adding magnetic impurities. This suggests an additional mechanism for the transverse relaxivity. We believe that this mechanism may result from the ferromagnetic impurities near or at the surface of the porous matrix, which cause extremely large magnetic field gradients at the pore surface, giving a rapid dephasing mechanism close to the pore wall. Normally in a CPMG measurement, dephasing can be refocused by the 180° pulses and will not enter into the value of the surface relaxation time. However, dephasing in extremely large magnetic field gradients may be difficult or impossible to rephase. Therefore we will interpret our experimental results in terms of a model in which a pore is divided into two different regions. In the region around the middle of the pore, an effective gradient is assumed to be present. Dephasing due to diffusion in this magnetic field gradient can be refocused with a CPMG pulse sequence with an interpulse time of 160 μs. At the pore wall, a much larger magnetic field gradient is present giving rise to an increase of the apparant surface relaxivity. Of course, these two regions are not sharply seperated but gradually merge into each other. It is not clear yet which fraction of the nuclear magnetization in the pores can effectively be refocused and which fraction will yield the

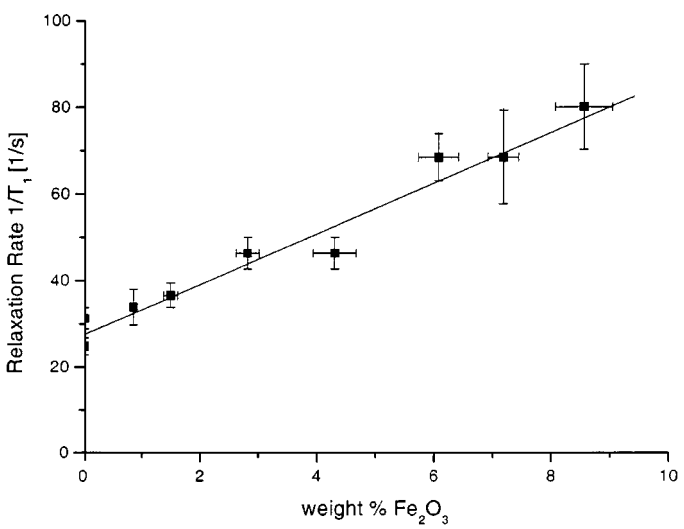

FIG. 4. Longitudinal relaxation rate as a function of the amount of magnetic impurities.

extra magnetization "surface sink" parameter. Therefore, the effect of this rapid dephasing mechanism at the pore wall is presently investigated with the aid of random walk simulations.

4. DIFFUSION AND DEPHASING

4.1. Regimes

Hürlimann (*12*) defined three length scales to characterize NMR diffusion measurements on porous materials:

1. the diffusion length, $l_D = \sqrt{D_0 \tau}$, where D_0 is the molecular self-diffusion coefficient (2.3×10^{-9} m^2/s for water at room temperature);
2. the size of the pore, $l_S = V/S$, where V is the volume and S is the surface of the pore;
3. the dephasing length, $l_g = \sqrt[3]{D_0(\gamma g)}$, where γ is the gyromagnetic ratio (for ^{1}H, $\gamma/2\pi = 42.6$ MHz/T) and g is the magnetic field gradient.

The dephasing part of the Hahn spin-echo decay due to diffusion can be associated with one of three asymptotic regimes. The shortest of the above-defined length scales (l_D, l_S or l_g) determines the regime.

The best known regime is the free diffusion regime. In this regime, the diffusion length is the shortest length scale. During the spin-echo sequence, the majority of the spins have not yet diffused far enough to hit a pore wall. The dephasing part of the spin-echo decay was already described by Hahn (*13*):

$$E_d = \exp\left(-\frac{1}{12} D_0 (\gamma g)^2 \cdot (2\tau)^3\right). \qquad [5]$$

When the diffusion time τ increases, the spins are going to feel the effect of the restricted geometry. There are two possibilities. They may first hit the wall, in which case the pore size l_S is the smallest length scale. The dephasing part of the spin-echo decay is then described by the motional averaging regime. For a fluid confined between two parallel plates (*14*) (*15*) have calculated that

$$E_d = \exp\left(-\frac{1}{120} \frac{(\gamma g)^2 l_S^4}{D_0} \cdot 2\tau\right). \qquad [6]$$

Other geometries will lead to another numerical prefactor (*16*).

The other possibility is that the individual spins dephase at least 2π before they can reach the wall. In this case, the dephasing length l_g is the smallest length scale. The dephasing part of the spin-echo decay is then described by the localization regime. For a fluid confined between two parallel plates, the following equation has been obtained (*17*):

$$E_d = \exp\left(-1.02(\gamma g)^{2/3} D_0^{1/3} \cdot 2\tau\right). \qquad [7]$$

An exact solution for a three-dimensional situation is not available.

It is clear (*12*) that intermediate regimes may exist if the above-defined length scales are about the same. However, no description of the dephasing behavior has been reported for these intermediate situations. Moreover, a real porous material will not have isolated pores of exactly the same size, but interconnected pores and also a broad pore size distribution may be present.

4.2. Dephasing Measurement

In order to study the effect of the internal magnetic field gradients on the dephasing of the NMR signal, Hahn spin-echo measurements were performed. The time τ between the 90° and the 180° pulses was varied. The Hahn spin-echo signal, however, is also attenuated by relaxation effects (See Eq. [3]). In principle, one could use CPMG measurements to correct for these effects, but in our clay samples such measurements may be affected by dephasing effects even for the smallest interpulse spacing of 160 μs. The longitudinal relaxation time, on the other hand, is not affected by dephasing. It is also known from a number of studies on relaxation rates in porous materials, that T_1 varies between T_2 and $2T_2$ (*18*). Therefore, the relaxation effect in the Hahn spin echo is estimated by three different methods, $T_{2,r} = T_{2,CPMG}$, $T_{2,r} = T_1$ and $T_{2,r} = 0.5 \times T_1$. To obtain $T_{2,d}$, the Hahn spin-echo intensity at 2τ is divided by $M_0 \cdot \exp(-2\tau/T_{2,r})$ for all three estimates.

Figure 5 shows the results for the sample with no extra magnetic impurities for all three relaxation estimates. It can be seen that the difference in the three sets of results is not large. The dephasing part shows a nearly mono-exponential decay. Only the data before $t = 2$ ms deviate from the linear fit. This time

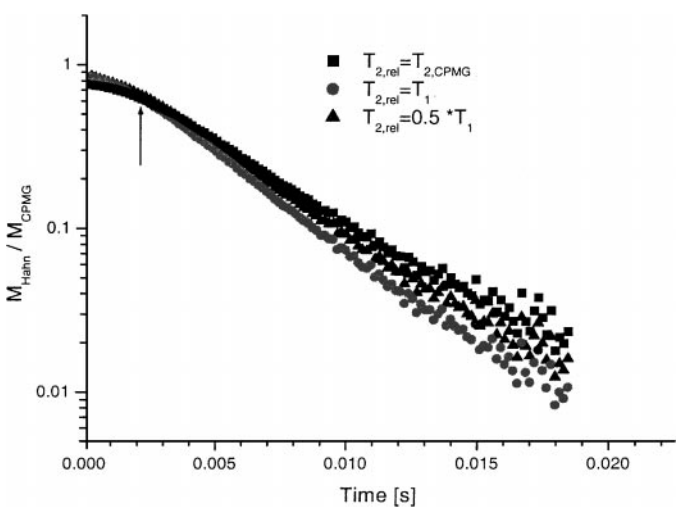

FIG. 5. Dephasing part of the spin-echo decay for the Kaolin clay sample with no extra Fe_2O_3. The solid squares correspond to a correction with a CPMG measurement; the solid circles correspond to a correction with T_1; the solid triangles correspond to a correction with $0.5 \cdot T_1$. Before time $t = 2$ ms (arrow), the measurements are assumed to be in the free diffusion regime.

corresponds to a diffusion length of about 5 μm, which is of the same order as the typical pore size. Before this time, the majority of the spins do not reach the restriction of the pore wall and are therefore described by the free diffusion regime. After $t = 2$ ms the spins are described either by the localization, the motional averaging, or an intermediate regime, because these regimes have a mono-exponential diffusion behavior. This succession of free and restricted diffusion was found only for the sample with no extra Fe_2O_3. All doped clay samples showed a mono-exponential dephasing behavior from $t = 160$ μs (the minimum spin echo time). The difference between the results obtained from the three relaxation estimates is larger for these doped samples. This will be discussed in more detail in the next section.

The maximum magnetic field gradient that can be applied with our experimental setup is 0.3 T/m. Even at this maximum magnetic field gradient no change in spin-echo decay could be induced for the different samples. The only observed effect was a decrease of the signal intensity with increasing gradient strength. This is obvious because we use only one gradient, which acts both as slice selection and readout gradient. Therefore with increasing gradient strength, the thickness of the selected slice decreases. The insensitivity of the signal decay to the externally applied gradient leads us to the conclusion that the internal magnetic field gradients are substantially larger than the externally applied magnetic field gradient.

To distinguish between the localization and the motional averaging regime, one must analyze the behavior of the spin-echo decay for a varying self-diffusion coefficient D_0 or a varying magnetic gradient strength g. First, we attempted to vary the self-diffusion coefficient D_0 by varying the temperature of the sample between 20° and 80°C. Since no significant differences in NMR relaxation and diffusion behavior were observed, we focussed our attention to the other variable in the dephasing expression.

As mentioned above, varying the external magnetic field gradient did not change the NMR spin-echo decay because of the dominant internal magnetic field gradients. However, the internal magnetic field gradients have actually been varied by preparing different samples with different concentrations of magnetic impurities. From the SQUID measurements, the magnetization of these samples is known.

4.3. Pore Model

We first neglect the large local gradients that may be present close to the Fe_2O_3 particles, and assume that the remaining pore region may be described by an effective magnetic field gradient. Brown and Fantazzini (*19*) showed that the variation in the effective local magnetic field is limited by $\Delta\chi B_0$. We prefer to deduce this limit directly from the definition

$$\vec{B} = \mu_0(\vec{H} + \vec{M}). \qquad [8]$$

Since in our experiments $\vec{M}$ is directed along $\vec{B}_0$, the demagnetizing field ΔB at the pore surface equals zero when $\vec{B}$ is perpendicular to the pore wall, or $\mu_0 M$ when $\vec{B}$ is parallel to the pore wall. Other orientations of $\vec{B}$ yield demagnetizing fields in between these extreme values. Assuming that the magnetization of the porous material itself is uniform, the maximum variation of the magnetic field inside the pores amounts to $\mu_0 M$, where M is the magnetization at the main magnetic field $B_0 = 0.8$ T. The maximum variation occurs at distances comparable to the typical pore size l_S. Hence the magnitude of the effective internal magnetic field gradient can be estimated by

$$g = \frac{\mu_0 M}{l_S}. \qquad [9]$$

One should note that, although quantitatively this estimate for g is rather crude, the actual magnitude of g in our series of samples will scale with M, since these samples have the same pore geometry. Substitution of this effective internal magnetic field gradient g into the equation for the dephasing part of the decay in the motional averaging regime (Eq. [6]) gives

$$E_d = \exp\left(-\frac{1}{120}\frac{l_S^2}{D_0}\cdot(\gamma\mu_0 M)^2\cdot 2\tau\right), \qquad [10]$$

whereas substitution into the equation for the dephasing part of the decay in the localization regime (Eq. [7]) yields

$$E_d = \exp\left(-1.02\frac{D_0^{1/3}}{(l_S)^{2/3}}\cdot(\gamma\mu_0 M)^{2/3}\cdot 2\tau\right). \qquad [11]$$

To be able to distinguish between the localization and the motional averaging regime, we write the decay due to dephasing as a mono-exponential function and consider the decay rate R_d

$$E_d = \exp(-R_d\cdot\tau). \qquad [12]$$

In Fig. 6, the experimental data on the decay rate R_d is plotted on a log–log scale as a function of the magnetization M. Because we introduced three relaxation estimates, we obtained three possible decay rates. To keep this figure clear, we only plotted the average result of the three methods. The vertical error bars reflect the difference between the methods. If we take a linear fit through the data with the CPMG measurement correction, the slope will be 0.57 ± 0.06. The T_1 correction will give a slope of 0.75 ± 0.06 and the $0.5 \cdot T_1$ correction will give a slope of 0.72 ± 0.06. It was observed that the two latter corrections yield nearly the same decay rate. A linear fit through the averaged data (as shown in Fig. 6) yields a slope of 0.66 ± 0.06. Also plotted in Fig. 6 are lines with slope 1 and

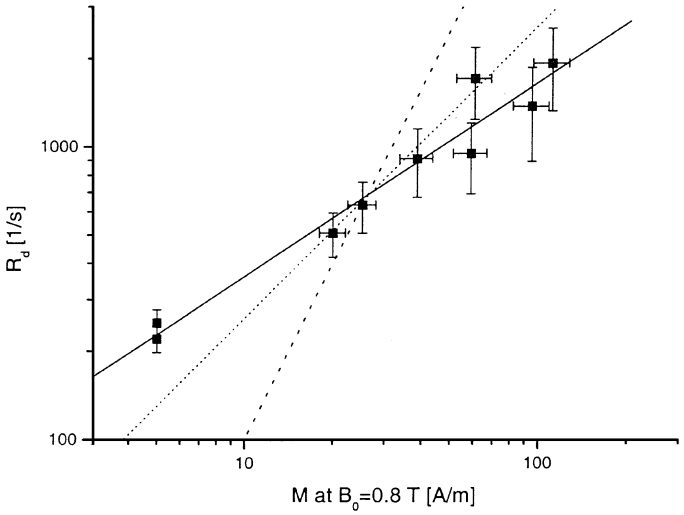

FIG. 6. Decay rate R_d describing the dephasing as a function of the magnetization M at a main magnetic field strength $B_0 = 0.8$ T. The transverse relaxation rate is estimated by three different methods. The average result for every sample is plotted as a function of the magnetization. The error bars are derived from the difference of the three methods. A linear fit through the data yields a slope of 0.66 ± 0.06. The dashed line has a slope 1 corresponding to the "linear regime"; the dotted line has a slope 2, corresponding to the motional averaging regime.

slope 2. Inspection of the figure shows that the dephasing cannot be modeled by the motional averaging regime (Eq. [10]), which would result in a M^2-dependence. A good candidate would be the localization regime (Eq. [11]), which has a $M^{2/3}$-dependence. However, also a linear M-dependence could be possible within the uncertainty of the measurements. This dependence would correspond to an intermediate regime and was also found by Borgia *et al.* (*20*). They found that R_d is both linear with magnetization and frequency. This "linear regime" is characterized by a Cauchy phase distribution of the spin particles, which would result from a random distribution of dipole moments. We already mentioned that the surface layer in our pore is characterized by large magnetic field inhomogeneities. These can be caused by the Fe_2O_3 particles at or near the pore surface, which act as strong magnetic dipole moments. For example, a Fe_2O_3 particle with a radius of 1 μm, which is 1 μm inside the clay material, will give a magnetic field gradient at the pore wall of about 7000 T/m. Phase accumulation during even the shortest spin echo time (160 μs) in such a high magnetic field gradient may yield a phase shift of about several tens of radians. In the presence of random motion such an enormous dephasing generally cannot be refocused. Fortunately, the dipole magnetic field contribution falls off with the third power of the distance and the magnetic field gradient even with the fourth power. Therefore in the inner part of the pore the dipole fields from the individual Fe_2O_3 particles are very likely one or two orders of magnitude smaller and will partly cancel. A description of this region in terms of an effective gradient may be appropriate.

4.4. Effective Gradient Pore Part

As discussed above, it is likely that the inner part of the pore can still be described by an effective gradient. For this part of the pore, we can estimate some length scales and magnetic field strengths. If we substitute the observed values of R_d (Eq. [27]) in Eq. [7] for the localization regime, we obtain an effective gradient of about 2 T/m for the clay sample with no extra Fe_2O_3 impurity and about 20 T/m for the clay sample with maximum (8 wt% Fe_2O_3) impurity. These effective gradients cause dephasing lengths l_g between 3.2 μm (no extra Fe_2O_3 impurity) and 1.4 μm (8 wt% Fe_2O_3 impurity). Because our experimental results indicate that the dephasing length must be smaller than or about equal to the pore size, this gives a lower limit of 3.2 μm for the pore size l_S. On the other hand, if we estimate the internal effective gradients from Eq. [9], taking $l_S = 3.2$ μm, we obtain effective internal gradients varying between 2 (no Fe_2O_3) and 44 T/m (8 wt% Fe_2O_3). Given the crudeness of this approximation and the limited validity of the effective gradient model for the inner part of the pore, these values agree nicely with those obtained above.

5. CONCLUSIONS

The typical pore size of the clay samples is determined by different techniques, which all give consistent results. The typical pore size measured with the PID-technique is between 1 and 10 μm. Analysis of the SEM images confims this estimate. The transition from free diffusion to restricted diffusion in the NMR measurement on the pure Kaolin clay sample suggests a typical pore size of about 5 μm. The measured dephasing lengths suggest that the typical pore size is larger than 3.2 μm.

Magnetization measurements with a SQUID magnetometer show that the Kaolin clay sample is paramagnetic and the Fe_2O_3 doped Kaolin clay samples have a ferro- and paramagnetic contribution. The total magnetization depends linearly on the amount of Fe_2O_3 impurity. Because of the ferromagnetic contribution, one can better use the total magnetization than the more commonly used magnetic susceptibility for describing the NMR dephasing due to diffusion in the magnetic fields of the clay pores.

The magnetic impurities in Fe_2O_3-doped Kaolin clay dominate both the longitudinal and, to a larger extent, the transverse relaxation. The impurities enhance the relaxation of water molecules that are hitting the pore surface. This so-called surface relaxivity is found to vary linearly with the magnetic impurity concentration. The transverse relaxivity depends much stronger on the magnetic impurity concentration than the longitudinal relaxivity, indicating that an extra transverse relaxation mechanism is present in the doped clay samples.

The Hahn spin echo measurements have a signal decay resulting from the combination of relaxation effects and dephasing due to diffusion in an inhomogeneous magnetic field. The transverse relaxation effect can be estimated by the decay of a CPMG

measurement with an as small as possible interpulse time or by relating it to the longitudinal relaxation time. If the measured spin echo intensity is divided by one of these estimates of the transverse relaxation time, the dephasing part can be extracted from a Hahn spin echo measurement. Such analysis show that the internal magnetic field gradients in the clay samples are substantially larger than the externally applied gradient of 0.3 T/m. This holds even for the clay sample with no additional Fe_2O_3. The spin echo decay due to dephasing of all the clay samples is described by an intermediate "linear regime" or the localization regime.

All these measurements lead to the following model of the pores in the Kaolin clay samples. The surface layer of the pore (not necessarily a mono-layer) is influenced by the magnetic dipole fields from the Fe_2O_3 impurities. Within a distance of about 1 μm, local magnetic field gradients can be larger than 1000 T/m. Dephasing in these fields cannot be refocused and will effectively lead to an extra transverse relaxation effect. The influence of the dipole falls off rapidly with increasing distance. Therefore, the inner part of the pore can be described by an effective gradient of the order of 1 or 10 T/m. Of course, the division of the pore into two regions with different magnetic field gradients is a simplification: in the actual system a transition region will exist.

ACKNOWLEDGMENTS

The authors thank J. Noijen for technical assistance with the NMR equipment, G. Strijkers and B. Smit for their help with the SQUID magnetometer, S. v.d. Sande for his help with the PID-measurements, H. Dalderop for his help with the preparation of the clay samples and SEM images, and R. Vlaardingerbroek for stimulating discussions. Part of this project is supported by the Dutch Technology Foundation (STW).

REFERENCES

1. S. Bhattacharja, W. P. Halperin, F. D'Orazio, and T. C. Tarczon, *in* "Magnetic Resonance Relaxation Analysis of Porous Media," Chap. 11, p. 311, Wiley, New York (1989).
2. L. Pel, K. Kopinga, G. Bertram, and G. Lang, Water absorption in a fired-clay brick observed by NMR scanning, *J. Phys. D: Appl. Phys.* **28,** 675–680 (1995).
3. T. W. Bremner, P. J. Prado, D. P. Green, R. L. Armstrong, S. D. Beyea, B. J. Balcom, and P. E. Grattan-Bellew, Magnetic resonance imaging and moisture content profiles of drying concrete, *Cem. Concr. Res.* **28,** 453–463 (1998).
4. P. Fantazzini, G. C. Borgia, and R. J. S. Brown, Nuclear magnetic resonance relaxivity and suface-to-volume ratio in porous media with a wide distribution of pore sizes, *J. Appl. Phys.* **79,** 3656–3664 (1996).
5. K. R. Brownstein and C. E. Tarr, Importance of classical diffusion in NMR studies of water in biological cells, *Phys. Rev. A* **19,** 2446–2452 (1979).
6. M. H. Cohen and K. S. Mendelson, Nuclear magnetic relaxation and the internal geometry of sedimentary rocks, *J. Appl. Phys.* **53,** 1127–1135 (1982).
7. Kleinberg, "Nuclear Magnetic Resonance," Vol. 35, Chap. 9, pp. 337–385, Academic Press, San Diego (1999).
8. H. Y. Carr and E. M. Purcell, Effects of diffusion on free precession in nuclear magnetic resonance experiments, *Phys. Rev.* **94,** 630–638 (1954).
9. E. M. Purcell, N. Bloembergen, and R. V. Pound, Relaxation effects in nuclear magnetic resonance absorption, *Phys. Rev.* **73,** 679–712 (1948).
10. D. L. Johnson, K. R. McCall, and R. A. Guyer, Magnetization evolution in connected pore systems, *Phys. Rev. B* **44,** 7344–7355 (1991).
11. C. J. Daughney, T. R. Bryar, and R. J. Knight, Paramagnetic effects of iron (III) species on nuclear magnetic relaxation of fluid protons in porous media, *J. Magn. Reson.* **142,** 74–85 (2000).
12. M. D. Hürlimann, Effective gradients in porous media to susceptibility differences, *J. Magn. Reson.* **131,** 232–240 (1998).
13. E. L. Hahn, Spin echoes, *Phys. Rev.* **80,** 580–594 (1950).
14. R. C. Wayne and R. M. Cotts, Nuclear-magnetic-resonance study of self-diffusion in a bounded medium, *Phys. Rev.* **151,** 264–272 (1966).
15. B. Robertson, Spin-echo decay of spins diffusing in a bounded region, *Phys. Rev.* **151,** 273–277 (1966).
16. C. H. Neuman, Spin echo of spins diffusing in a bounded medium, *J. Chem. Phys.* **60,** 4508–4511 (1974).
17. T. M. De Swiet and P. N. Sen, Decay of nuclear magnetization by bounded diffusion in a constant field gradient, *J. Chem. Phys.* **100,** 5597–5604, (1994).
18. S. A. Farooqui, R. L. Kleinberg, and M. A. Horsfield, T1/T2 ratio and frequency dependence of NMR relaxation in porous sedimentary rocks, *J. Colloid Interface Sci.* **158,** 195–198 (1993).
19. R. J. S. Brown and P. Fantazzini, Conditions for initial quasilinear 1/t2 versus tau for Carr–Purcell–Meiboom–Gill NMR with diffusion and susceptibility differences in porous media and tissues, *Phys. Rev. B* **47,** 14823–14834 (1993).
20. R. J. S. Brown, G. C. Borgia, and P. Fantazzini, Scaling of spin-echo amplitudes with frequency, diffusion coefficient, pore size, and susceptibility difference for the NMR of fluids in porous media and biological tissues, *Phys. Rev. E* **51,** 2104–2114 (1995).